Science of the Total Environment 729 (2020) 138798

Contents lists available at ScienceDirect

Science of the Total Environment

journal homepage: www.elsevier.com/locate/scitotenv

Indoor air partitioning of Synthetic Musk Compounds: Gas, particulate matter, house dust, and window film

Esin Balci [a], Mesut Genisoglu [a], Sait C. Sofuoglu [a], Aysun Sofuoglu [b,*]

[a] Izmir Institute of Technology, Dept. of Environmental Engineering, Urla, Turkey
[b] Izmir Institute of Technology, Dept. of Chemical Engineering, Urla, Turkey

HIGHLIGHTS

- Gas and particle SMC concentrations showed a similar trend with time.
- Gas – PM_{10} and gas – window film SMC concentrations were correlated.
- Gas – dust and gas – window film partitioning coefficient values were correlated.
- SMCs found in gas phase and partition to PM_{10}, dust, and window film.
- Unaccounted surfaces were most probably significant reservoirs for SMCs.

GRAPHICAL ABSTRACT

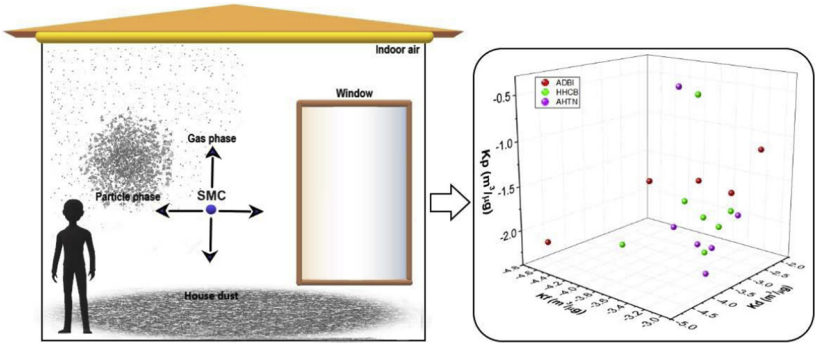

ARTICLE INFO

Article history:
Received 24 January 2020
Received in revised form 16 April 2020
Accepted 17 April 2020
Available online 21 April 2020

Keywords:
Synthetic Musk Compounds
Polycyclic musks
Nitro musks
Partitioning
Indoor environment

ABSTRACT

Due to diversity of contaminants indoors and complexity in the physical structure of particulate matter, partition process of chemicals affects indoor concentration distribution. Synthetic Musk Compounds (SMCs) are ubiquitously found in household and personal care products, thus, in the environment. Exposure to SMCs is important for human health, therefore, their partitioning in indoor environmental media is a key issue. In this study, gas – particle, house dust, and window film partitioning of SMCs were investigated in an indoor micro-environment. In a sealed and unoccupied room, a polycyclic and nitro musk mixture was left for volatilization for an hour. Then, samples were collected using XAD-2 sandwiched between two PUF plugs, glass-fiber filter, and wipes for gas, PM_{10}, window-film, house dust phases, respectively, for 145 h. Collected samples were analyzed using a GC–MS. Results demonstrated that SMC concentrations decreased over time, non-linearly. Six of the SMCs partitioned to PM_{10} with at least 10% at beginning of the experiment, whereas the number of compounds dropped to two at the end, showing that SMCs may partition well between the two phases but they tend to be in the gas phase. They were also detected in the film and dust phases but a decrease pattern similar to gas-particle was not observed. Spearman correlations indicate that the dust and film-associated concentrations were governed by similar processes but PM-associated concentrations were not. SMCs may be found in all phases, mainly in house dust in terms of mass among the studied media and unaccounted surface reservoirs. Therefore, their partitioning between indoor media has key implications for human exposure.

1. Introduction

Synthetic Musk Compounds (SMCs) have been produced in large quantities as a substitute of expensive and unsustainable natural

* Corresponding author.
E-mail address: aysunsofuoglu@iyte.edu.tr (A. Sofuoglu).

https://doi.org/10.1016/j.scitotenv.2020.138798
0048-9697/

musks obtained from animals and fragrant plants. SMCs have been widely used all over the world as fragrance in consumer products such as air fresheners, household and personal care products. Concerns about the biological and environmental effects of SMCs have begun in 1980s after their presence in freshwater fish samples was reported for the first time (Yamagishi et al., 1983). Then, their occurrence has been investigated in all environmental media with increasing attention (e.g., Peck and Hornbuckle, 2004; Xie et al., 2007; Rubinfeld and Luthy, 2008; McDonough et al., 2016). They have also been detected in biota (Draisci et al., 1998; Nakata et al., 2015) and in human biological samples including adipose tissue (Kannan et al., 2005; Schiavone et al., 2010), breast milk (Liebl and Ehrenstorfer, 1993; Lignel et al., 2008), and blood (Hutter et al., 2005; Hu et al., 2010).

Structurally, SMCs are classified as nitro (NMs), polycyclic (PCMs), macrocyclic (MCMs), and alicyclic musks (ACMs). Nitro musks, which are alkylated nitrobenzene derivatives, exhibit similar physical and chemical properties to persistent organic pollutants (POPs) having a wide range of transport ability, resistance, and bioaccumulation capacity in the environment. The five most commercially relevant NMs are Musk Ketone (MK), Musk Ambrette (MA), Musk Moskene (MM), Musk Tibetene (MT), and Musk Xylene (MX). The use of MM and MT are banned in cosmetics in some countries because of skin related problems and allergic reactions (Chisvert et al., 2018). MA has been discontinued from use due to photosensitivity and neurotoxicity issues (Taylor et al., 2014; Li et al., 2018). MX and MK were the most commonly used NMs. However, under the Regulation on Registration, Evaluation, Authorization and Restriction of Chemicals (REACH), MX was classified as a substance that is highly resistant, and bioaccumulative. International Fragrance Association (IFRA), banned the use of MX, and European Commission followed the ban due to its potential adverse impacts (IFRA, 2011). In addition, use of MK was limited in the US because of its bioaccumulative properties. NMs have largely been replaced by PCMs due to bans/restrictions in several countries. Compared with NMs, PCMs have higher resistance to light and alkali environments. They include Galaxolide (HHCB), Tonalide (AHTN), Celestolide (ADBI), Phantolide (AHMI), Traseolide (ATII), Cashmeran (DPMI). AHTN and HHCB are the most commercially-used PCMs (95%) (Gatermann et al., 2002). Both of the compounds were identified as high production volume chemicals by the US Environmental Protection Agency (USEPA), and added to the Hazardous Substances Data Bank and Toxicology Data Network. Because the other two groups of SMCs (MCMs and ACMs) have been recently introduced into the market, they are not used as much as PCMs. Although the levels and fate of SMCs in different matrices have been extensively studied, knowledge about their distribution in the indoor environment is very limited. Consumer products used in households constitute an important source of contamination for the indoor residential environment (Weschler and Nazaroff, 2008).

They exist in both in the gas and particle phases due to their semi-volatile properties (Weschler and Nazaroff, 2008). In turn, considering the high particle binding-affinity of SMCs, the indoor dust may be a reservoir and important source of exposure (Butte, 2004; Lu et al., 2011; Liu et al., 2013). Therefore, their partitioning between indoor environmental media is crucial for human exposure. SMCs were mainly found to be in the gas phase both in a primary school classroom and a women's sport center in our previous study (Sofuoglu et al., 2010). Although the proportion was similar (>95%), a higher number of SMCs (ADBI, AHTN, ATII, HHCB, and MX) were detected in the classroom $PM_{2.5}$ compared to that in the sports center (HHCB, AHTN, and ATII). HHCB and AHTN were reported to be detected in about half of the PM_{10} samples collected in French dwellings with concentrations of up to 95th percentile values of 759 and 377 pg/m^3 (Mandin et al., 2016). HHCB and AHTN were the most detected SMCs in cosmetics, health care, and cleaning products while banned compounds (MA and MT) were also detected according to a recent review (Lucattini et al., 2018). Reviews show that HHCB was detected in all collected indoor dust samples in the US (Mitro et al., 2016) and was the most frequently detected SMC at relatively higher concentrations (Lucattini et al., 2018). Gaseous indoor air concentrations were reported to be in the order of ng/m^3 for HHCB and AHTN in various micro-environments in France, Germany, Spain, and Turkey (Lucattini et al., 2018). Therefore, exposure through indoor air which is one of the most human-exposure-relevant environments is of critical importance. House dust and gaseous phases are the preferred indoor media for the study of SMCs in the literature, while there is little information on their partitioning to particulate matter and window film. This study aimed to investigate partitioning of SMCs between gas – particulate, gas – window film and gas – house dust phases experimentally in an indoor environment. In addition, their occurrence was investigated in window films in 10 offices in the building.

2. Material and methods

2.1. Materials

A standard comprising ADBI, AHMI, AHTN, ATII, DPMI, and HHCB as PCMs, and MA, MK, MT, and MX as NMs was purchased from Neochema GmbH & Co.KG (Bodenheim, Germany). Gas chromatographic grade ethyl acetate, acetone, n-hexane, and dichloromethane (Suprasolv; Merck, Germany) were used for the clean-up, extraction, and GC–MS applications. After extraction of samples, Florisil (100–200 mesh; Sigma-Aldrich, USA) and anhydrous sodium sulfate (Fluka, Steinheim, Germany) were used. Florisil was preferred for cleaning pesticide residues, other chlorinated hydrocarbons and for separating nitrogen compounds from hydrocarbons and aromatic compounds from aliphatic-aromatic mixtures and similar applications for use with oils, fats and waxes (USEPA, 2007) while anhydrous sodium sulfate was used for the removal of any water residue.

2.2. Sampling

Prior to the experiment, the floor was cleaned with vacuum and mop to remove old dust. Windows were cleaned using isopropyl alcohol, acetone, and hexane to remove old film layer. Then, the window and floor area were divided into sections for sequential sampling. The room was kept unoccupied for one month for regrowth of window film and settled dust. Musk mixture prepared to contain ~46 μg of DPMI, ADBI, AHMI, ATII, AHTN, HHCB, MA, MK, MX, and MT, was placed in a glass petri dish on top of a hotplate and left to volatilize for 1 h in an unoccupied room (L × W × H of 6.10 × 2.90 × 3.80 m). A ventilator was operated during the 1-h period at a low speed for a better mixing in the room of which windows were kept closed and the door was sealed. Gas and particulate phase samples were collected with an active air sampling system consisted of a Harvard impactor (Air Diagnostics & Engineering Inc., Harrison, ME, USA), in which a 37-mm glass-fiber filter (1 μm pore) was placed in the impactor to capture PM with aerodynamic diameter <10 μm at 10 L/min flow rate, Amberlite XAD-2 resin sandwiched between polyurethane foam (PUF) plugs (Supelco, Bellefonte, USA) in a glass holder followed to collect gas phase sample, connected to a vacuum pump (Air Diagnostics & Engineering Inc., SP-280). Five 4-h samples were collected in the first day of the experiment followed by 24-h samples collected at 2nd, 3rd, 4th, and 6th days. The experiment lasted for 145 h. Flow rate at the start of each sample was set to 10 L/min, and measured at the end to determine if the difference is <10% required to deem the sample acceptable. Window film and settled dust samples were collected simultaneously with gas-PM sampling using pro-wipe (non-woven propylene, Pro-Wipe 880, Berkshire). Pro-wipes were pre-cleaned using ultrasonic extraction with acetone:hexane before sampling. Pre-cleaned pro-wipes were dried at 50 °C using vacuum oven. Dried pro-wipes were wrapped with aluminum foil and kept at −20 °C in zippered bag until the sampling. Pro-wipes were moistened with isopropyl alcohol (IPA) for sampling using a 0.40 m × 0.41 m template for settled dust and window film.

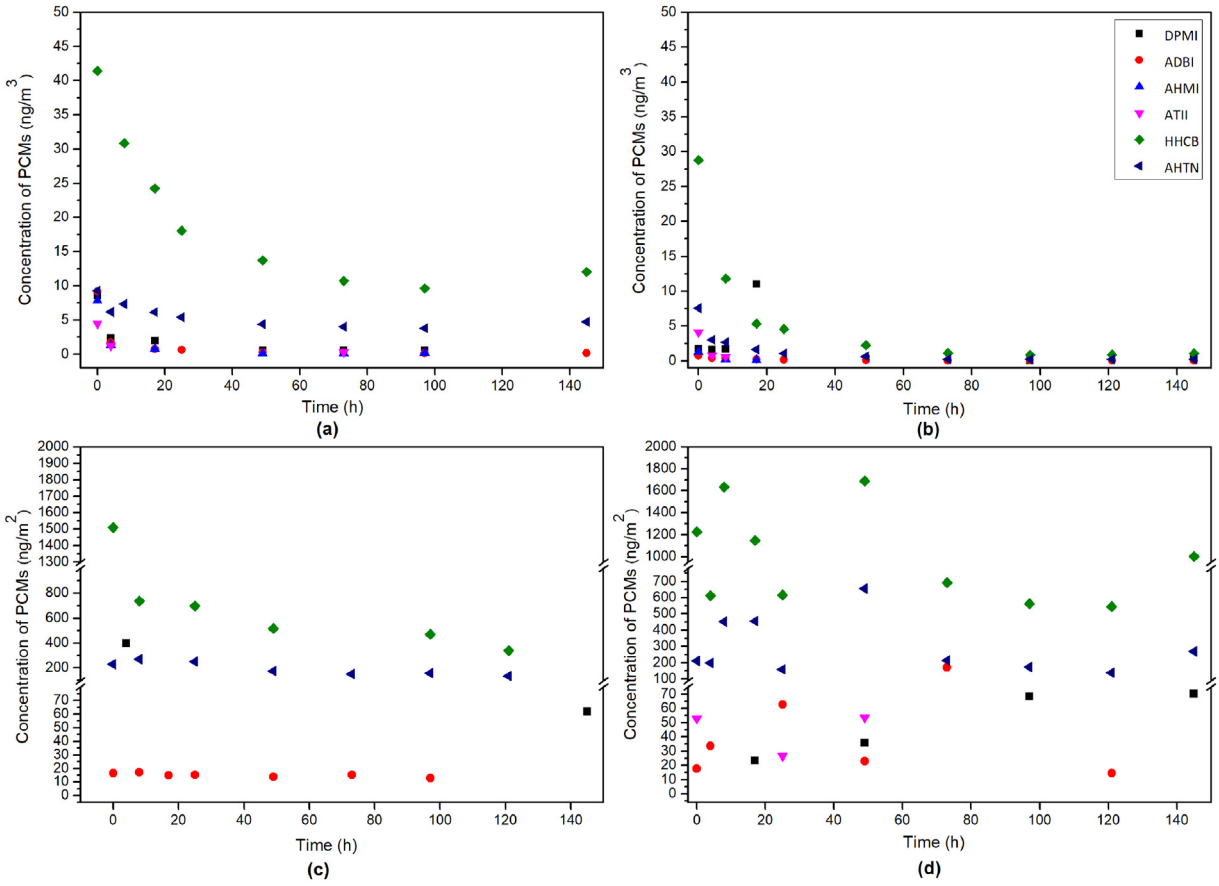

Fig. 1. Concentrations of PCMs in (a) gas, (b) particle (c) window film, and (d) house dust phases during the experiment.

2.3. Sample processing

Before extraction, fluoranthene-d10 (F_{d10}) surrogate standard solution was added to the samples (50 pg/μL concentration). Afterwards, samples were ultrasonically extracted for 30 min with an acetone:hexane mixture (1:1 v/v). Then, under a nitrogen gas flow of 100 mL/min the volume was reduced to 5 mL. Next, 10 mL of hexane was added three times to change the solvent to hexane. Finally, the volume was reduced to 2 mL. For clean-up, a chromatographic column prepared by placing a piece of glass wool, 0.75 g Florisil and 1 cm sodium anhydrous sulfate into a Pasteur glass pipet. Prior to column chromatography, Florisil and sodium anhydrous sulfate were activated in the oven at 650 °C and 450 °C, respectively. Before Florisil was placed in the column, its deactivation was performed by adding water. Firstly, the samples were passed through the column and discharged. After 4 mL of ethyl acetate was passed the column, solvent phase samples were collected in amber vials. Volume of the samples was reduced to 1 mL under a gentle nitrogen gas flow. Then, solvent was changed into hexane and the extracts were stored at −20 °C until GC–MS analysis.

2.4. Analysis

A GC–MS, equipped with DB-5MS (30 m × 0.25 mm × 0.25 μm) capillary column and programmable-temperature-vaporizing injection, was used in EI mode for separation and quantification of SMCs, operated in selective ion monitoring (SIM) mode. Helium was used as a carrier with the flow rate of 1 mL/min. Oven program was 60 °C 1 min hold time, 15 °C/min ramp to 180 °C, 0.2 °C/min to 185 °C and 30 °C/min to 250 °C with 6 min hold time. MS transfer line and ion source temperatures were 250 and 230 °C, respectively. Programmable temperature vaporization (PTV) mode was used to inject the samples. Inlet temperature program was started at 100 °C with the duration of 0.05 min and the temperature was increased to 250 °C with the ramp of 14.5 °C and hold for 2 min. Monitored ions of DPMI were 191 and 206; ADBI and AHMI were 229 and 244, MA were 253 and 268, ATII were 215 and 258, HHCB were 213 and 243, AHTN were 243 and 258, MX were 282 and 297, MM were 263 and 278, MT were 251 and 266, MK were 278, 279, and 294.

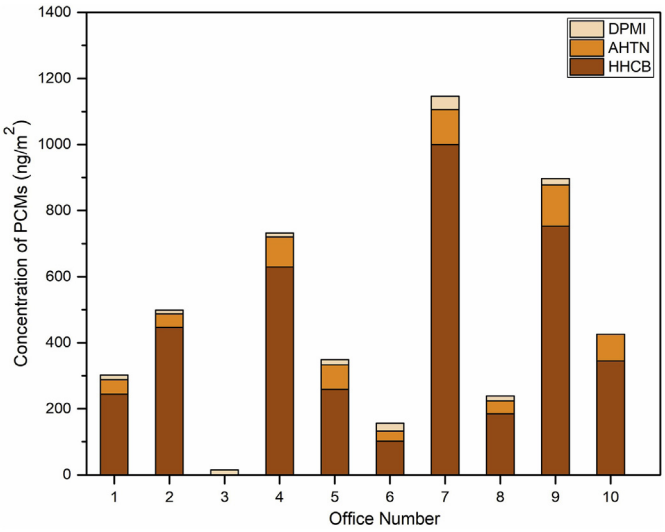

Fig. 2. Window-film PCM concentrations in the 10 offices.

2.5. QA/QC

All glasswares were rinsed with acetone and hexane after cleaning with ultrapure water. Aluminum foils were baked at 450 °C. Samples were stored at −20 °C in a zippered bag until the extraction. Amber glassware was used for protection of samples from UV light. 50 ng each of SMCs were spiked to Pro-wipes (triplicate) and processed like a sample to determine recoveries. The average (spike) recoveries of SMCs were determined to be 69%, 96%, 94%, 85%, 101%, 70%, 81%, 103%, 111%, 108%, 74% for DPMI, ADBI, AHMI, MA, ATII, HHCB, AHTN, MX, MM, MT, and MK, respectively. Method Detection Limits were estimated to range from 0.03 to 0.14 ng/m^3 for gas and particle phases, 3.05 to 15.2 ng/m^2 for window film and house dust.

2.6. Partitioning

The partitioning of SMCs between particle and gas phases can be characterized by particle/gas partition coefficient (K_P) (Pankow, 1994; Weschler and Nazaroff, 2008) using Eq. (1).

$$K_P = \left(\frac{C_P}{C_{PM10}}\right)/C_G \quad (1)$$

where, C_P (ng/m^3) is the SMC concentration in the particulate matter, C_{PM10} (μg/m^3) is the PM_{10} concentration, and C_G (ng/m^3) is the SMC concentration in the gas phase.

Dust-gas (K_D) and window film-gas (K_F) partitioning behavior of SMCs were determined using Eq. (2) (Weschler and Nazaroff, 2008). It was assumed that the particulates forming the film layer on the window surface exhibit similar partitioning behaviors as the settled dust. Mass of window film and house dust were determined prior to the experiment with three samples taken with the template. The average was used in Eq. (2).

$$K_{D\text{ or }F} = \frac{X_{D\text{ or }F}}{C_G} \quad (2)$$

where, K_D (m^3/μg) is the dust-gas partition coefficient, K_F (m^3/μg) is the window film-gas partition coefficient, X_D (ng/μg) is the settled dust SMC concentration, X_F (ng/μg) is the window film SMC concentration.

3. Results and discussion

3.1. PCM concentrations

At the start of the experiment (in the first 4-h period) gas phase concentrations were determined to be 8.55, 9.14, 7.88, 4.49, 41.4, and 9.30 ng/m^3, respectively for DPMI, ADBI, AHMI, ATII, HHCB, and AHTN (Fig. 1a). At the end of the experiment (in the final 24-h period, the 6th day), gas phase concentrations were decreased to 0.18, 12.03, and 4.72 ng/m^3 for ADBI, HHCB, and AHTN, respectively, while the remaining compounds were below the detection limit (BDL). At the start of the experiment, PM_{10}-bounded DPMI, ADBI, AHMI, ATII, HHCB, and AHTN concentrations were determined to be 1.79, 0.74, 1.28, 4.10, 28.8, and 7.55 ng/m^3, respectively, whereas at the end, particle-phase DPMI, ADBI, HHCB, and AHTN were found to be 0.28, 0.07, 1.07, and 0.22 ng/m^3, respectively, while the others were BDL (Fig. 1b). At the start of the experiment, window-film concentrations were measured as 397, 16.5, 1511, and 229 ng/m^2, respectively, for DPMI, ADBI, HHCB and AHTN. At the end of the experiment, they were decreased to 61.8,

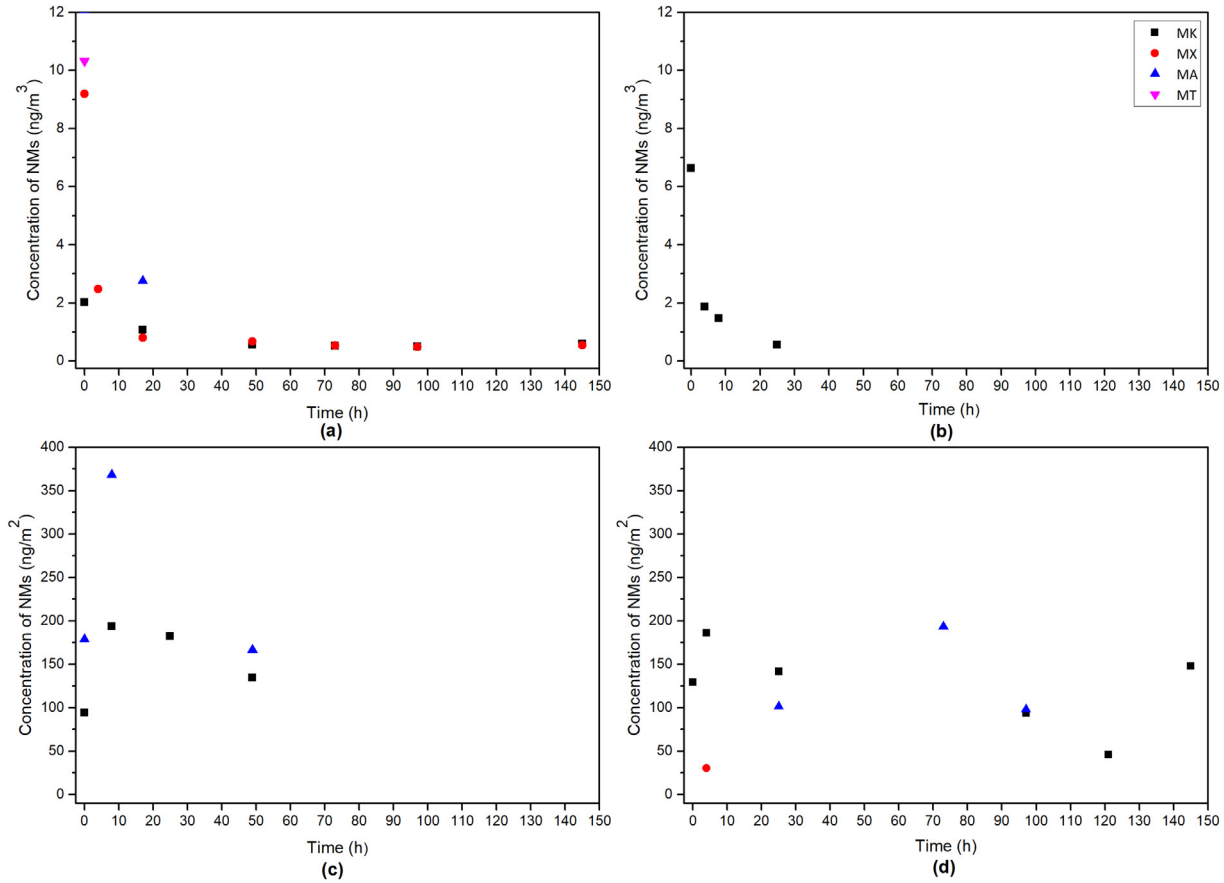

Fig. 3. Concentrations of NMs in (a) gas, (b) particle, (c) window film, and (d) house dust during the experiment.

339, and 135 ng/m^2 for DPMI, HHCB, and AHTN, respectively, while ADBI was BDL. On the other hand, house dust DPMI and AHTN concentrations did not decrease from the start to the end of experiment (Fig. 1d). The decrease pattern in gas and particle-phase concentrations indicated similarity, which was apparent in the highest-concentration compounds (AHTN and HHCB). Window-film and house-dust concentrations showed a similar pattern that is different than the gas and particle phases. In fact, there was a visible decrease in window-film concentration for only HHCB while the others stayed at the same level. Concentrations in house dust did not show a decrease for any of the compounds, in which there is actually a visible fluctuation. The reason for this may be (1) heterogeneity in accumulated dust with in the sampled floor area. Mass-based concentrations were not measured to avoid volatilization of target analytes during weighing. In addition, the surfaces available for SMCs to partition (gypsum-board ceiling tiles, walls, and furniture, a desk and a bookcase made of MDF boards) were not accounted. The ceiling tiling, was reported to be a sink for VOCs (Thevenet et al., 2018).

The mean PCM concentrations in window film samples collected from the 10 randomly-selected offices were 440 ± 297, 70.3 ± 33.6, and 18.3 ± 8.92 ng/m^2 for HHCB, AHTN, and DPMI, respectively. As can be seen from Figs. 1c and 2, HHCB was the highest concentration PCM in window film samples and the average concentration in offices and the concentration at the end of the experiment (339 ng/m^2) are at a similar level. Variation in office PCM concentrations may be related to the musk contents of the products used in the office and by the office occupier.

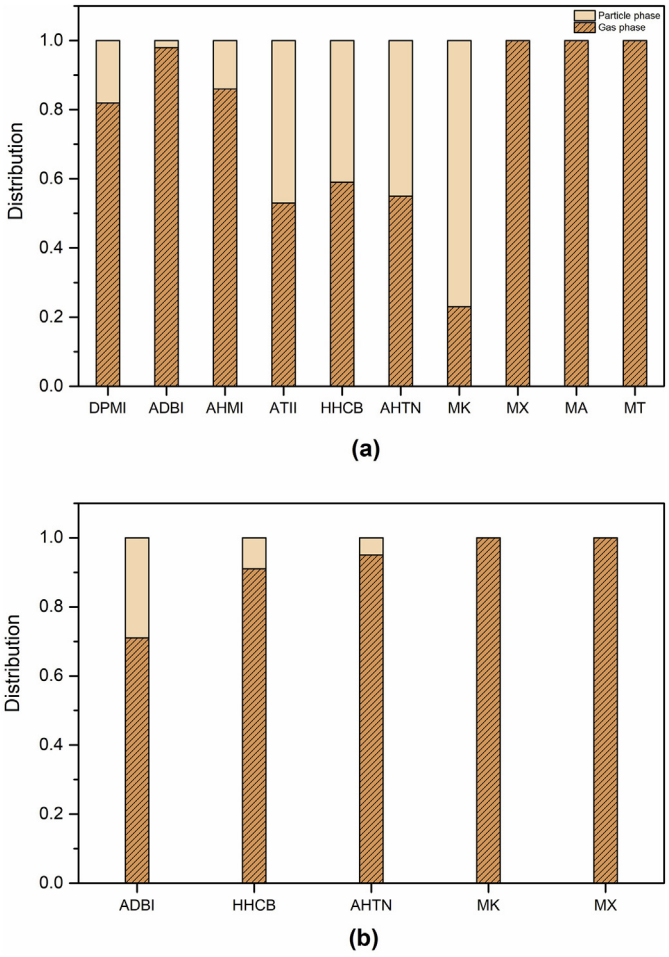

Fig. 4. Gas – particle partitioning of SMCs during (a) the first 4 h and (b) the final 24 h.

3.2. NM concentrations

At the beginning of the experiment, all of NMs were observed in the gas phase (Fig. 3a). Their concentrations were determined to be 2.02, 9.20, 12.1, and 10.3 ng/m^3, respectively for MK, MX, MA, and MT. At the end of the experiment, only MK and MX were detectable at 0.58 and 0.53 ng/m^3, respectively. MA and MT were BDL before the end of the first day. As shown in Fig. 3b, only MK could be found in the particle phase at the beginning, which also was BDL after 48 h. At the start of the experiment, window film concentrations were determined to be 179 and 94.3 ng/m^2, respectively for only MA and MK (Fig. 3c). Furthermore, the concentrations first increased before decreasing in window film and house dust probably because 1 h was not sufficient to reach their adsorption capacity. At the end of the experiment, no compound was detectable in window film while only MK was detected in house dust (Fig. 3d). The other NMs were generally determined to be BDL possibly due to the spiked amount to the room was not sufficient to increase NMs in airborne particles, tendency to be in gas phase, and partitioning to the unaccounted reservoir surfaces (Fig. 4a and b). Also, the experimental confounding mentioned for PCMs may had a role on the house dust concentrations. Window-film NM concentrations were all BDL in the 10 offices.

Similarity in the concentrations and profiles found for polycyclic aromatic hydrocarbons (PAHs) in indoor window film and indoor dust samples were explained with equilibrium differences among PAHs (Huo et al., 2016). In general SMC concentrations showed similarity between gas-particle and dust-window film, probably due to differences in variables that determine partitioning, such as physicochemical properties, particle characteristics, and environmental conditions.

3.3. Gas/particle partitioning

In this study, unlike the start of the experiment, the SMCs were found to be at a higher proportion in the gas phase than the particle phase at end of the experiment. Chen et al. (2007) investigated presence and distribution of PCMs in a typical cosmetic plant in China, and reported that they were dominantly found in the gas phase. Our previous study (Sofuoglu et al., 2010) reported higher gas-phase concentrations than the particle ($PM_{2.5}$) in a primary school classroom and a women's sport center. HHCB and AHTN were reported to be detected in about half of the PM_{10} samples collected in French dwellings with concentrations of up to 95th percentile values of 759 and 377 pg/m^3, respectively, but with the median values of BDL, <42 and <21 pg/m^3, respectively (Mandin et al., 2016). Weinberg et al. (2011) investigated SMCs released from a wastewater treatment plant to air. Although, all SMCs were observed in the gas phase, ATII, MX, and MT were not detected in the particle phase, while HHCB and AHTN were found in both phases. Nevertheless, the authors underlined that most of SMCs dominated in gas phase, with particle phase being <1% of the total musk concentration except for AHMI and ADBI in some samples.

As shown in Fig. 4a, DPMI, AHMI, ATII, HHCB, and AHTN of PCMs, and only MK of NMs were found in both of the phases in the first 4 h of the experiment, while MX, MA, and MT were all in the gas phase. Fig. 4b, on the other hand, shows that ADBI, HHCB, AHTN, MK, and MX were dominantly in the gas phase, while DPMI could not be detected in the gas phase at the 6th day. However, DPMI concentration in the gas phase was detectable at 0.56 ng/m^3, while its particle phase concentration (0.07 ng/m^3) was close to the BDL (0.14 ng/m^3) at the 5th day. As a result, DPMI was detectable on the particulate phase at the end of the experiment.

This study was carried out with a spiked concentration increase in the experiment. The concentrations generally decreased with time. The concentrations measured along the experiment may correspond to real-life conditions where concentrations increase with the use SMC containing household and personal care products. Therefore, values of the partitioning coefficients may be useful for the scientific community. The statistics of partitioning coefficients determined for the time steps of

Table 1
Descriptive statistics of the SMC partitioning coefficient values.

		N[a]	Mean	SD[b]	CV[c]	Min	Q1[d]	Median	Q3[e]	Max	IQR[f] (Q3 -Q1)	Range (Max-Min)
$LogK_P$ (m^3/μg)	DPMI	6	−1.34	0.56	−0.42	−2.00	−1.71	−1.45	−0.94	−0.50	0.77	1.50
	ADBI	8	−1.51	0.33	−0.22	−2.13	−1.68	−1.46	−1.27	−1.13	0.41	1.00
	AHMI	2	−1.53	0.68	−0.44	−2.02	−2.02	−1.53	−1.05	−1.05	0.96	0.96
	MA	0	–	–	–	–	–	–	–	–	–	–
	ATII	2	−1.01	1.00	−0.99	−1.71	−1.71	−1.01	−0.30	−0.30	1.41	1.41
	HHCB	9	−1.78	0.57	−0.32	−2.44	−2.12	−1.85	−1.72	−0.42	0.41	2.02
	AHTN	9	−1.77	0.57	−0.32	−2.38	−2.09	−1.84	−1.77	−0.35	0.32	2.03
	MX	0	–	–	–	–	–	–	–	–	–	–
	MT	0	–	–	–	–	–	–	–	–	–	–
	MK	1	0.25	–	–	–	–	–	–	–	–	–
$LogK_D$ (m^3/μg)	DPMI	4	−3.48	0.49	−0.14	−3.94	−3.89	−3.53	−3.07	−2.92	0.82	1.02
	ADBI	6	−3.44	0.88	−0.25	−4.73	−3.91	−3.40	−3.03	−2.18	0.87	2.54
	AHMI	0	–	–	–	–	–	–	–	–	–	–
	MA	0	–	–	–	–	–	–	–	–	–	–
	ATII	1	−3.94	–	–	–	–	–	–	–	–	–
	HHCB	10	−3.41	0.36	−0.10	−4.01	−3.54	−3.31	−3.20	−2.92	0.34	1.09
	AHTN	10	−3.34	0.25	−0.07	−3.66	−3.54	−3.32	−3.22	−2.84	0.32	0.81
	MX	1	−3.92	–	–	–	–	–	–	–	–	–
	MT	0	–	–	–	–	–	–	–	–	–	–
	MK	3	−2.85	0.32	−0.11	−3.21	−3.21	−2.74	−2.61	−2.61	0.60	0.60
$LogK_F$ (m^3/μg)	DPMI	2	−3.09	0.63	−0.20	−3.53	−3.53	−3.09	−2.64	−2.64	0.89	0.89
	ADBI	6	−3.47	0.64	−0.18	−4.60	−3.69	−3.31	−3.09	−2.81	0.60	1.79
	AHMI	0	–	–	–	–	–	–	–	–	–	–
	MA	1	−3.69	–	–	–	–	–	–	–	–	–
	ATII	0	–	–	–	–	–	–	–	–	–	–
	HHCB	8	−3.41	0.26	−0.08	−3.99	−3.47	−3.36	−3.23	−3.15	0.24	0.83
	AHTN	7	−3.32	0.15	−0.04	−3.52	−3.46	−3.29	−3.21	−3.10	0.25	0.42
	MX	0	–	–	–	–	–	–	–	–	–	–
	MT	0	–	–	–	–	–	–	–	–	–	–
	MK	3	−2.66	0.46	−0.17	−3.19	−3.19	−2.44	−2.34	−2.34	0.84	0.84

[a] Number of samples.
[b] Standard deviation.
[c] Coefficient of variation.
[d] First quartile.
[e] Third quartile.
[f] Interquartile range.

the experiment are presented in Table 1. According to our measurements, the PM_{10} concentration varied from 5.95 μg/m^3 to 33.7 μg/m^3 during the experiment. $logK_P$ values based on the measured SMC concentrations in this study were calculated to be −0.94, −1.35, −1.05, −0.30, −0.42, −0.35, and 0.25 m^3/μg for DPMI, ADBI, AHMI, ATII, HHCB, AHTN, and MK, respectively, during the first 4 h of the experiment. At the end of the experiment, $logK_P$ values could be calculated for only ADBI, HHCB, and AHTN to be −1.18, −1.82, and −2.10 m^3/μg, respectively, due to the BDL compounds. However, this value of DPMI was determined as −1.99 m^3/μg in the 4th day. In addition, $logK_P$ values of SMCs ranged from −2.00 to −0.50 m^3/μg for DPMI, from −2.13 to −1.13 m^3/μg for ADBI, from −2.44 to −0.42 m^3/μg for HHCB, and from −0.32 to −0.35 m^3/μg for AHTN. The mean $logK_P$ values of HHCB and AHTN were estimated to be −3.80 and −3.78 m^3/μg, respectively, based on K_{OA}, while the maximum values (−2.61 for AHTN and −2.42 for HHCB) were closer to those measured in this study (Wei et al., 2016).

3.4. Gas/window-film partitioning

The average window film amount was determined as 11.77 mg. $logK_F$ based on the concentrations measured at the start of the experiment were calculated to be −4.60, −3.29, −3.46, and −3.19 m^3/μg for ADBI, HHCB, AHTN, MA, and MK, respectively. At the end of the experiment, $logK_F$ value of HHCB, and AHTN were determined to be −3.41 and −3.40 m^3/μg, respectively. Although, this value for the other compounds was not calculated due their concentrations being BDL, $logK_F$ value of ADBI and MK in the 3rd day was determined to be −3.11 and −2.44 m^3/μg, respectively. $logK_F$ values of HHCB and AHTN ranged from −3.99 to −3.15 m^3/μg, and from −3.52 to −3.10 m^3/μg, respectively. The average $logK_F$ values were determined to be −3.09, −3.47, −3.69, −3.41, −3.32, and −2.66 m^3/μg for DPMI, ADBI, MA, HHCB, AHTN, and MK, respectively. Relatively low Coefficient of Variation (CV) value of AHTN and HHCB might indicate that partitioning of these two SMCs were not influenced by the studied concentration levels as the remaining SMCs.

In the literature, the discussions on equilibrium in partitioning onto indoor window film and dust mainly based on correlation between octanol-air partition coefficient (K_{OA}) and dust/film ($K_{D/F}$) partition coefficients. However, it is reported that a compound's $logK_{OA}$ value can be used to estimate theoretical $logK_D$. If measured $logK_D$ values were comparable to the theoretical values, it can be elaborated that there is an equilibrium (Weschler and Nazaroff, 2010; Li et al., 2019). Unfortunately, there is no measured K_{OA} values for SMCs. In addition, the molar mass, boiling point, saturation vapor pressure and octanol/air

Table 2
Spearman correlation coefficients (and p-values) of HHCB concentrations.

	Gas phase	PM	Dust	Window film
Gas phase	1	0.93 (<0.01)	0.2 (0.58)	0.71 (0.04)
PM	0.93 (<0.01)	1	0.52 (0.10)	0.80 (0.01)
Dust	0.20 (0.58)	0.52 (0.10)	1	0.70 (0.04)
Window film	0.71 (0.04)	0.80 (0.01)	0.70 (0.04)	1

Table 3
Spearman correlation coefficients (and p-values) of AHTN concentrations.

	Gas phase	PM	Dust	Window film
Gas phase	1	0.93 (<0.01)	−0.05 (0.88)	0.48 (0.23)
PM	0.93 (<0.01)	1	0.14 (0.69)	0.53 (0.14)
Dust	−0.05 (0.88)	0.14 (0.69)	1	0.40 (0.29)
Window film	0.48 (0.23)	0.53 (0.14)	0.40 (0.29)	1

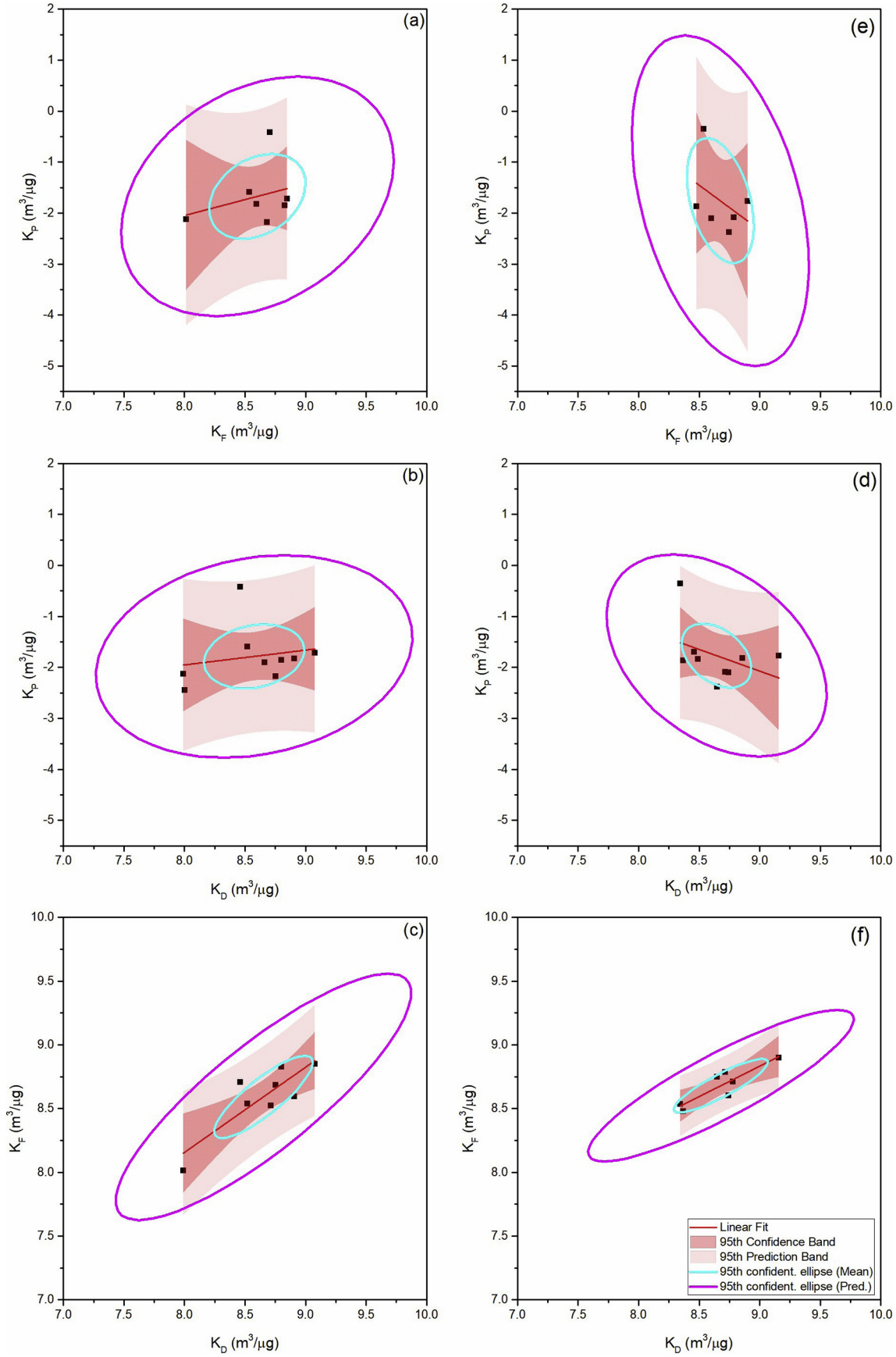

Fig. 5. Simple Linear Regression between partition coefficients for (a–c) HHBC and (d–f) AHTN.

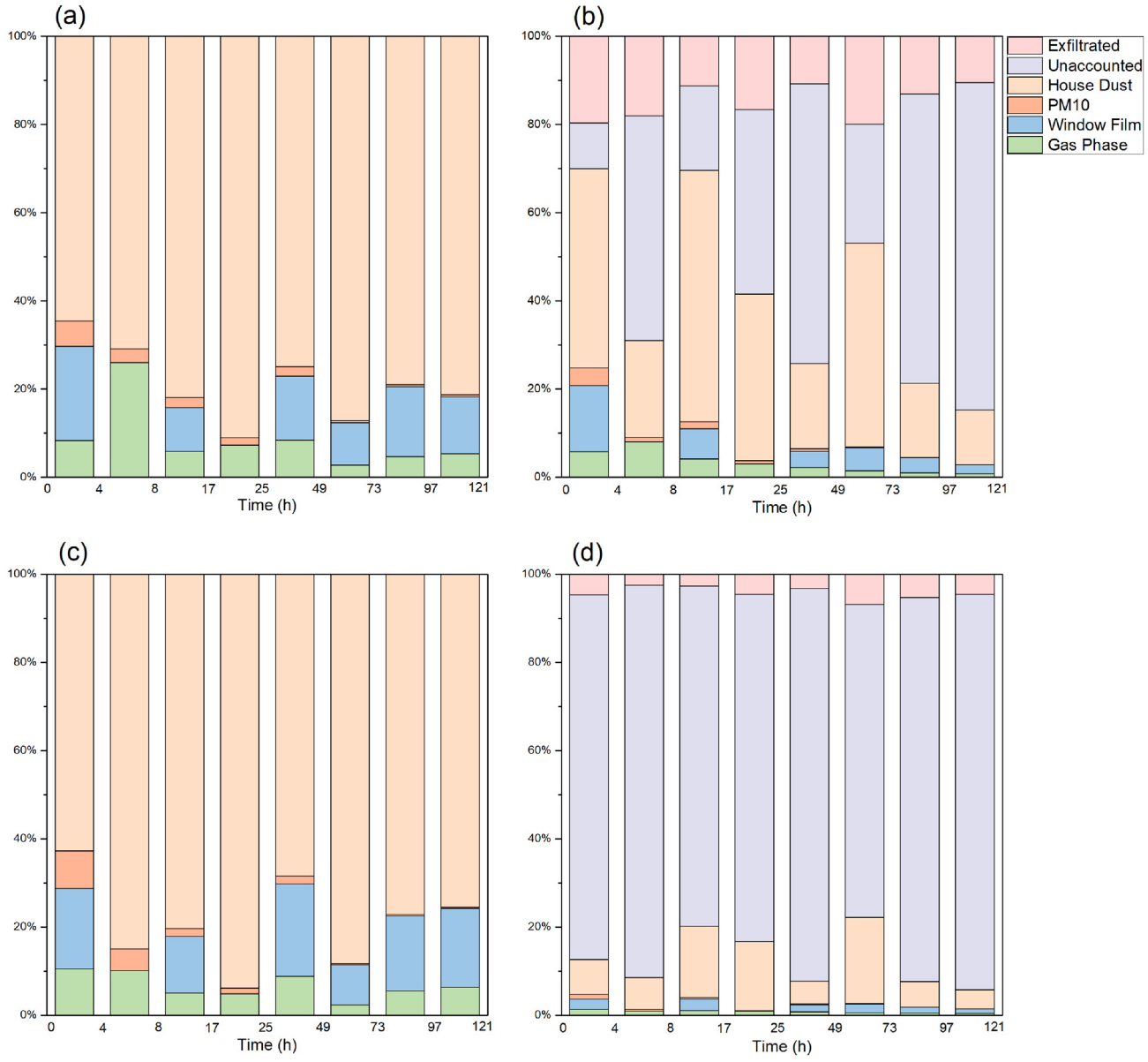

Fig. 6. Distribution of mass during the experiment for (a) HHCB and (c) AHTN among the studied media, and for (b) HHCB and (d) AHTN including exfiltration and unaccounted media.

partition coefficient were reported as important parameters on the partitioning of compounds (Wei et al., 2019).

3.5. Gas/dust partitioning

The average house dust amount was determined to be 16.88 mg for the template area. $\log K_D$ value of ADBI, ATII, HHCB, AHTN, and MK were determined to be −4.73, −3.94, −3.54, −3.66, and −3.21 $m^3/\mu g$ respectively. At the end of the experiment, $\log K_D$ values of HHCB, AHTN and MK were determined to be −3.10, −3.25 and −2.60 $m^3/\mu g$, respectively. Meanwhile, $\log K_D$ value for the other compounds was not calculated due to the fact that their concentrations were BDL. However, this value for DPMI and ADBI was determined as −2.18 $m^3/\mu g$ in the 4th day and −2.92 $m^3/\mu g$ in the 3rd day, respectively. $\log K_D$ values of HHCB, AHTN, and MK ranged from −4.01 to −2.92 $m^3/\mu g$, from −3.66 to −2.84 $m^3/\mu g$, and from −3.20 to −2.60 $m^3/\mu g$, respectively. The average $\log K_D$ values were determined to be −3.48, −3.44, −3.94, −3.41, −3.34, −3, 92, and −2.85 $m^3/\mu g$ for DPMI, ADBI, ATII, HHCB, AHTN, MX, and MK, respectively. CV values of HHCB and AHTN were relatively lower than the others similar to $\log K_F$ values.

3.6. Multiple linear regression analysis

Multiple linear regression (MLR) analysis was used to study relationship of concentrations between gas, particulate, window film, and dust phases. MLR could only be conducted on HHCB and AHTN concentrations due to the lacking matching data between the four phases. Gas phase concentration was selected as the dependent variable and the others were independent variables. The model for HHCB concentrations explained the variation in the data set well (adjusted $R^2 = 0.95$; $p = 0.001$). Adequacy measures (normality, constant variance, and independence of residuals, and the R^2 value) confirmed the adequacy of the constructed MLR model. The model, the ANOVA table, and results of residual analysis are presented in the SM (Table SM-1, Figs. SM-1–SM-4). The most contributing variable was particle concentration. Removing window film concentration from the independent variables still resulted in a significant model ($p < 0.04$) with an adjusted R^2 value of 0.48,

while removing house dust from independent variables again resulted in a significant ($p < 0.0001$) model with an adjusted R^2 value of 0.93. Spearman correlation was used to assess relationship between concentration phases since the normality was rejected for HHCB concentrations (Table 2). Gas and particulate phase and gas and window film phase concentrations were highly correlated with the correlation coefficient values of 0.92 and 0.70, respectively. However, settled dust HHCB concentrations were not correlated with gas phase ($r = 0.20$), while they were correlated to window film concentrations ($r = 0.70$). Adjusted R^2 value of the MLR analysis of AHTN concentrations was determined to be 0.87. The model was significant with a p-value of 0.0098. Adequacy measures (normality, constant variance, and independence of residuals, and the R^2 value) confirmed the adequacy of the constructed MLR model. The model, the ANOVA table, and results of residual analysis are presented in the SM (Table SM-1, Figs. SM-1–SM-4). The most contributing variable was the particle-phase concentration. Removing the dust concentration and the window film concentration from the independent variables still resulted in a significant model ($p < 0.0001$) with an R^2 value of 0.88. Spearman correlation coefficients of AHTN concentrations between phases are shown in Table 3. Similar correlation coefficient (0.93) between gas and particulate phases was determined for AHTN. However, correlation coefficient of gas and window film phases (0.48) was lower than that of HHCB. House dust AHTN concentrations have no correlation with the gas phase. The correlation between window film and house dust phases was lower than those of HHCB.

Linear regression was also used to determine the relationship between partitioning values of HHCB and AHTN (Fig. 5). A significant relationship was determined between K_D and K_F with an R^2 value of 0.71 for HHCB and 0.77 for AHTN. However, the linear relationship between the K_P-K_D and K_P-K_F were determined to be weak with $R^2 < 0.15$. Intercept, slope and R^2 values of the linear models are listed in the SM (Table SM-2). Spearman correlation coefficients were also calculated because the non-parametric test does not require the assumption of normality. The analysis indicated a strong relationship between K_D and K_F of HHCB ($r = 0.64$) and AHTN ($r = 0.68$) (Tables SM-3 and -4). Spearman correlation coefficient of K_P-K_D and K_P-K_F were <0.28. The correlations indicate that house dust and window film associated concentrations were governed by similar processes but PM associated concentrations were not. However, gas and particle phase concentrations of HHCB and AHTN were determined to be strongly correlated (Tables 2 and 3), which indicate partitioning between the two phases was governed with similar processes.

3.7. Mass balance

Air exchange rate (AER, h^{-1}) of the room was determined based on the concentration decay method (Turanjanin et al., 2014). Dry ice was used as the source of the tracer gas (CO_2) for determining the AER. Indoor and outdoor (hallway) CO_2 levels of sealed and unsealed rooms were recorded with Quest EVM 7 (3M). AER of sealed and unsealed rooms were modeled to be 0.56 and 1.81 h^{-1}, respectively. The average AER of homes in summer, when our study was also conducted, was modeled to be 2.88 h^{-1} using CO_2 as a tracer gas (Bekö et al., 2016) while, residential ventilation is considered low below AER of 0.5 h^{-1} (Dimitroulopoulou, 2012). Sealing did not completely stop the dilution of the SMCs in the room, but significantly decreased AER (from 1.81 h^{-1} to 0.56 h^{-1}). Thus, partitioning of SMCs took place along with a relatively slow dilution caused by infiltration.

SVOCs were predicted to rather reside in condensed-phase materials than in gas phase by partitioning to the organic films on indoor surfaces especially for compounds with log K_{OA} values larger than about 5 or 6, and by diffusing into building materials and furnishings such as wallboard, paint, gypsum-board ceiling tiles (Weschler and Nazaroff, 2008; Thevenet et al., 2018; Wang et al., 2020). SMCs are such compounds with predicted log K_{OA} values ranging from 6.7 to 9.07 for PCMs and 7.8 to 12 for NMs (Wong et al., 2019). A mass balance was carried out to assess the effect of infiltration and partitioning to the media that were unaccounted in this study. HHCB and AHTN were selected for this purpose because concentrations of the remaining compounds were either low or BDL in a considerable portion of the samples. Percentages of mass partitioned to the studied media are presented in Fig. 6(a) and (c) for HHCB and AHTN, respectively, showing that both were dominantly in the house dust through the experiment followed by window film and gas phase. Including the mass removed by exfiltration and determining the percentage bound to unaccounted surface reservoirs (paint, wallboard, flooring and ceiling tiles, furnishings, etc.) resulted in a mass balance for HHCB and AHTN shown in Fig. 6(b) and (d), respectively. Percentages partitioned to the indoor media and removed by exfiltration remained fairly steady through the experiment for AHTN, whereas there were three distinguishable stages for HHCB. In the first 4 h, HHCB was mainly partitioned to house dust. Between 4th and 73rd h percentages for house dust, unaccounted reservoirs, and exfiltration were comparable while towards the end of the experiment (after 73rd h) unaccounted surfaces dominated.

4. Conclusion

Partitioning is a complex mechanism in indoor environment due to presence of many different materials and contaminants. In this study, the distribution of SMCs in particle, house dust, and window film against time were investigated. It is found that gas and particle SMC concentrations decreased with time while SMCs in window film and dust did not show such a clear pattern. SMCs were found in gas phase, and partitioned to PM_{10}, dust, and window film. Six of the SMCs partitioned to PM_{10} with at least 10% at the beginning of the experiment with $\log K_P$ values ranging between −0.94 and 0.25 $m^3/\mu g$, whereas it dropped to two compounds at the end with $\log K_P$ values ranging from −2.10 to −1.18 $m^3/\mu g$. The average $\log K_F$ values ranged from −3.69 (HHCB) to −2.66 $m^3/\mu g$ (MK). Generally, house dust and window film showed similarity in partitioning. SMCs may be found in all phases, mainly in house dust in terms of mass among the studied media, and unaccounted surface reservoirs. Therefore, their partitioning between indoor media has key implications for human exposure.

CRediT authorship contribution statement

Esin Balci: Writing - original draft, Investigation, Formal analysis, Visualization. **Mesut Genisoglu:** Investigation, Formal analysis, Visualization. **Sait C. Sofuoglu:** Conceptualization, Resources, Methodology, Writing - review & editing. **Aysun Sofuoglu:** Conceptualization, Methodology, Resources, Project administration, Writing - review & editing.

Declaration of competing interest

The authors declare that they have no known competing financial interests or personal relationships that could have appeared to influence the work reported in this paper.

Acknowledgment

We thank İpek Özen and Ecem Çınar for collection of the window-film samples in the office rooms. We also thank Environmental Research Center of Izmir Institute of Technology for GC/MS analysis.

Appendix A. Supplementary data

Supplementary data to this article can be found online at https://doi.org/10.1016/j.scitotenv.2020.138798.

References

Bekö, G., Gustavsen, S., Frederiksen, M., Bergsoe, N.C., Kolarik, B., Gunnarsen, L., Toftum, J., Clausen, G., 2016. Diurnal and seasonal variation in air exchange rates and interzonal airflows measured by active and passive tracer gas in homes. Build. Environ. 104, 178–187. https://doi.org/10.1016/j.buildenv.2016.05.016.

Butte, W., 2004. Synthetic musks in house dust. In: Rimkus, G.S. (Ed.), Series Anthropogenic Compounds. Springer, Berlin, Heidelberg, pp. 105–121. https://doi.org/10.1007/b14127.

Chen, D., Zeng, X., Sheng, Y., Bi, X., Gui, H., Sheng, G., Fu, J., 2007. The concentrations and distribution of polycyclic musks in a typical cosmetic plant. Chemosphere 66, 252–258. https://doi.org/10.1016/j.chemosphere.2006.05.024.

Chisvert, A., López-Nogueroles, M., Miralles, P., Salvador, A., 2018. Perfumes in cosmetics: regulatory aspects and analytical methods. In: Salvador, A., Chisvert, A. (Eds.), Analysis of Cosmetic Products. Elsevier, pp. 225–248. https://doi.org/10.1016/B978-0-444-63508-2.00010-2.

Dimitroulopoulou, C., 2012. Ventilation in European dwellings: a review. Build. Environ. 47, 109–125. https://doi.org/10.1016/j.buildenv.2011.07.016.

Draisci, R., Marchiaava, C., Ferreti, E., Palleschi, L., Catellani, G., Anastasia, A., 1998. Evaluation of musk concentration of freshwater fish in Italy by accelerated solvent extraction and gas chromatography with mass spectrometric detection. J. Chromatogr. 814, 187–197. https://doi.org/10.1016/S0021-9673(98)00396-3.

Gatermann, R., Biselli, S., Hühnerfuss, H., Rimkus, G.G., Franke, D., Hecker, M., Kallenborn, R., Karbe, L., König, W.A., 2002. Synthetic musk in the environment. Part 2: enantioselective transformation of the polycyclic musk fragrances HHCB, AHTN, AHDI and ATII in freshwater fish. Arch. Environ. Contam. Toxicol. 42, 447–452. https://doi.org/10.1007/s00244-001-0042-1.

Hu, Z., Shi, Y., Niu, H., Cai, Y., Jiang, G., Wu, Y., 2010. Occurrence of synthetic musk fragrances in human blood from 11 cities in China. Environ. Toxicol. Chem. 29, 1877–1882. https://doi.org/10.1002/etc.258.

Huo, C.Y., Liu, L.-Y., Zhang, Z.-F., Ma, W.-L., Song, W.-W., Li, H.-L., Li, W.-L., Kannan, K., Wu, Y.-K., Han, Y.-M., Peng, Z.-X., Li, Y.-F., 2016. Phthalate esters in indoor window films in a Northeastern Chinese Urban Center: film growth and implications for human exposure. Environ. Sci. Technol. 50, 7743–7751. https://doi.org/10.1021/acs.est.5b06371.

Hutter, H.P., Wallner, P., Moshammer, H., Hartl, W., Sattelberger, R., Lorbeer, G., Kundi, M., 2005. Blood concentrations of polycyclic musks in healthy young adults. Chemosphere 59 (4), 487–492. https://doi.org/10.1016/j.chemosphere.2005.01.070.

IFRA, 2011. EU Regulation follows fragrance industry's voluntary global ban. https://ifrafragrance.org/news/eu-regulation-follows-fragrance-industry-s-voluntary-global-ban, Accessed date: 14 January 2020.

Kannan, K., Reiner, J.L., Yun, S.H., Perrota, E.E., Tao, L., Johnson-Restrepo, B., Rodan, B., 2005. Polycyclic musk compounds in higher trophic level aquatic organisms and humans from the United States. Chemosphere 61, 693–700. https://doi.org/10.1016/j.chemosphere.2005.03.041.

Li, X., Chu, Z., Yang, J., Li, M., Du, M., Zhao, X., Zhu, Z.J., Li, Y., 2018. Synthetic Musks: a class of commercial fragrance additives in personal care products (PCPs) causing concern as emerging contaminants. Adv. Mar. Biol. 81, 213–280. https://doi.org/10.1016/bs.amb.2018.09.008.

Li, H.L., Liu, L.Y., Zhang, Z.F., Ma, W.L., Sverko, E., Zhang, Z., Song, W.W., Sun, Y., Li, Y.F., 2019. Semi-volatile organic compounds in infant homes: levels, influence factors, partitioning, and implications for human exposure. Environ. Pollut. 251, 609–618. https://doi.org/10.1016/j.envpol.2019.05.048.

Liebl, B., Ehrenstorfer, S., 1993. Nitro musks in human milk. Chemosphere 27 (11), 2253–2260. https://doi.org/10.1016/0045-6535(93)90136-S.

Lignel, S., Darnerud, P.O., Aune, M., Cnattingius, S., Hajslova, J., Setkova, L., Glynn, A., 2008. Temporal trends of synthetic musk compounds in mother's milk and associations with personel use of perfumed products. Environ. Sci. Technol. 42, 6743–6748. https://doi.org/10.1021/es800626n.

Liu, N., Shi, Y., Xu, L., Li, W., Cai, Y., 2013. Occupational exposure to synthetic musks in barbarshops, compared with the common exposure in the dormitories and households. Chemosphere 93, 1804–1810. https://doi.org/10.1016/j.chemosphere.2013.06.027.

Lu, Y., Yuan, T., Yun, S.H., Wang, W., Kannan, K., 2011. Occurrence of synthetic musks in indoor dust from China and implications for human exposure. Arch. Environ. Contam. Toxicol. 60 (1), 182–189. https://doi.org/10.1007/s00244-010-9595-1.

Lucattini, L., Poma, G., Covaci, A., Boer, J., Lamoree, M.H., Leonards, P.E.G., 2018. A review of semi-volatile organic compounds (SVOCs) in the indoor environment: occurrence in consumer products, indoor air and dust. Chemosphere 201, 466–482. https://doi.org/10.1016/j.chemosphere.2018.02.161.

Mandin, C., Mercier, F., Ramalho, O., Lucas, J.P., Gilles, E., Blanchard, O., Bonvallot, N., Glorennec, R., Le Bot, B., 2016. Semi-volatile organic compounds in the particulate phase in dwellings: a nationwide survey in France. Atmos. Environ. 136, 82–94. https://doi.org/10.1016/j.atmosenv.2016.04.016.

McDonough, C.A., Helm, P.A., Muir, D., Puggioni, G., Lohmann, R., 2016. Polycyclic musks in the air and water of the lower Great Lakes: spatial distribution and volatilization from surface waters. Environ. Sci. Technol. 50, 11575–11583. https://doi.org/10.1021/acs.est.6b03657.

Mitro, S.D., Dodson, R.E., Adamkiewicz, G., Elmi, A.F., Tilly, M.K., Zota, A.R., 2016. Consumer product chemicals in indoor dust: a quantitavie meta-analysis of U.S. studies. Environ. Sci. Technol. 50 (19), 10661–10672. https://doi.org/10.1021/acs.est.6b02023.

Nakata, H., Hinosaka, M., Yanagimoto, H., 2015. Macrocyclic-, polycyclic- and nitromusks in cosmetics, household commodities and indoor dusts collected from Japan: implications for their human exposure. Ecotoxicol. Environ. Saf. 111, 248–255. https://doi.org/10.1016/j.ecoenv.2014.09.032.

Pankow, J.F., 1994. An adsorption model of gas/particle partitioning of organic compounds in the atmosphere. Atmos. Environ. 28 (2), 185–188. https://doi.org/10.1016/1352-2310(94)90093-0.

Peck, A.M., Hornbuckle, K.C., 2004. Synthetic musk fragrances in Lake Michigan. Environ. Sci. Technol. 38 (2), 367–372. https://doi.org/10.1021/es034769y.

Rubinfeld, S.A., Luthy, R.G., 2008. Nitromusk compounds in San Francisco Bay sediments. Chemosphere 73 (6), 873–879. https://doi.org/10.1016/j.chemosphere.2008.07.042.

Schiavone, A., Kannan, K., Horii, Y., Focardii, S., Corsolini, S., 2010. Polybrominated diphenyl ethers, polychlorinated napthalenes and polycyclic musk in human fat from Italy: comparison to polychlorinated biphenyls and organochlorine pesticides. Environ. Pollut. 158, 599–606. https://doi.org/10.1016/j.envpol.2009.08.011.

Sofuoglu, A., Kiymet, N., Kavcar, P., Sofuoglu, S.C., 2010. Polycylic and nitromusk in indoor air: a primary school classroom and a women's sport center. Indoor Air 20, 515–522. https://doi.org/10.1111/j.1600-0668.2010.00674.x.

Taylor, K.M., Weisskopf, M., Shine, J., 2014. Human exposure to nitro musks and the evaluation of their potential toxicity an overview. Environ. Health 13, 14. https://doi.org/10.1186/1476-069X-13-14.

Thevenet, F., Debono, O., Rizk, M., Caron, F., Verriele, M., Locoge, N., 2018. VOC uptakes on gypsum boards: sorption performances and impact on indoor air quality. Build. Environ. 137, 138–146. https://doi.org/10.1016/j.buildenv.2018.04.011.

Turanjanin, V., Vucicevic, B., Jovanovic, M., Mirkov, N., Lazovic, I., 2014. Indoor CO_2 measurements in Serbian schools and ventilation rate calculation. Energy 77, 290–296. https://doi.org/10.1016/j.energy.2014.10.028.

U.S. Environmental Protection Agency (USEPA), 2007. Method 3620C-Florisil Cleanup.

Wang, C., Collins, D.B., Arata, C., Goldstein, A.H., Mattila, J.M., Farmer, D.K., Ampollini, L., DeCarlo, P.F., Novoselac, A., Vance, M.E., Nazaroff, W.W., Abbatt, J.P.D., 2020. Surface reservoirs dominate dynamic gas-surface partitioning of many indoor air constituents. Sci. Adv. 6 (8), eaay8973. https://doi.org/10.1126/sciadv.aay8973.

Wei, W., Mandin, C., Blanchard, O., Mercier, F., Pelletier, M., Le Bot, B., Glorennec, P., Romalho, O., 2016. Distributions of the particle/gas and dust/gas partition coefficients for seventy-two-semi-volatile organic compounds in indoor environment. Chemosphere 153, 212–219. https://doi.org/10.1016/j.chemosphere.2016.03.007.

Wei, W., Mandin, C., Blanchard, O., Mercier, F., Pelletier, M., Le Bot, B., Glorennec, P., Ramalho, O., 2019. Semi-volatile organic compounds in French dwellings: An estimation of concentrations in the gas phase and particulate phase from settled dust. Sci. Total Environ. 650, 2742–2750. https://doi.org/10.1016/j.scitotenv.2018.09.398.

Weinberg, I., Dreyer, A., Ebinghaus, R., 2011. Wastewater treatment plant as sources of polyfluorinated compounds, polybrominated diphenyl ethers and musk fragrances to ambient air. Environ. Pollut. 159, 125–132. https://doi.org/10.1016/j.envpol.2010.09.023.

Weschler, C.J., Nazaroff, W.W., 2008. Semivolatile organic compounds in indoor environments. Atmos. Environ. 42, 9018–9040. https://doi.org/10.1016/j.atmosenv.2008.09.052.

Weschler, C.J., Nazaroff, W.W., 2010. SVOC partitioning between the gas phase and settled dust indoors. Atmos. Environ. 44, 3609–3620. https://doi.org/10.1016/j.atmosenv.2010.06.029.

Wong, F., Robson, M., Melymuk, L., Shunthirasingham, C., Alexandrou, N., Shoeib, M., Luk, E., Helm, P., Diamond, M.L., Hung, H., 2019. Urban sources of synthetic musk compounds to the environment. Environ. Sci. Processes Impacts 21, 74–88. https://doi.org/10.1039/c8em00341f.

Xie, Z., Ebinghaus, R., Temme, C., Heemken, O., Ruck, W., 2007. Air-sea exchange fluxes of synthetic polycyclic musks in the North Sea and the Arctic. Environ. Sci. Technol. 41 (16), 5654–5659. https://doi.org/10.1021/es0704434.

Yamagishi, T., Miyazaki, T., Horii, S., Akiyama, K., 1983. Synthetic musk residues in biota and water from Tama River and Tokyo Bay (Japan). Arch. Environ. Contam. Toxicol. 12 (1), 83–89. https://doi.org/10.1007/BF01055006.